DESIGN AND VERIFICATION OF FLUTTER SUPPRESSION CONTROL SYSTEMS BY MULTIDISCIPLINARY CO-SIMULATIONS

Giulio Romanelli* , **Tommaso Solcia***
***Politecnico di Milano**
romanelli@aero.polimi.it; solcia@aero.polimi.it

Keywords: *co-simulations, multi-fidelity, transonic flutter*

Abstract

Aircrafts are complex machines in which the overall performances are determined by the co-operation of several subsystems. For the design of modern aircraft, interaction between aerodynamics, structural dynamics, flight dynamics and active controls, is nowadays becoming more and more important, mainly due to the increasing dimensions, the weight savings, and the high flexibility of structures. Thus, subsystems frequencies are very close to each other, and coupled multidisciplinary co-simulations are needed to predict the aircraft performances, even in the preliminary design phase. In this work, a high-fidelity free software co-simulation environment is proposed to simulate coupled aerodynamics and structural dynamics problems. Such a platform is used to verify the performances of an active control system for flutter suppression designed by means of low-fidelity efficient tools.

1 Introduction

The improvement of aircraft performances by control system design is a well established research and industrial topic. Significant resources have been invested by the aerospace industry to improve the efficiency and environmental sustainability of modern aircraft by means of passive wing tip devices, e.g. winglets. An example of the industrial interest also for actively controlled aircrafts is the F-18 High Alpha Research Vehicle (HARV) [1].

The objective of the present work is to tackle the problem of active control system design for transonic flutter suppression and to propose a software toolbox capable of running high-fidelity multidisciplinary co-simulations to verify the feasibility of the designed system, based on Computational Fluid Dynamics (CFD). This choice closely matches today's design best practices in the aerospace industry [2] [3] [4] .

The approach can be summarized as follows. In the first part an active control system is designed using a very computationally efficient linear low-fidelity model which can be embedded into an automatic optimization scheme (in this case a genetic algorithm is used). In the second part, the most promising concept is verified by means of high-fidelity models, resorting to CFD and Multibody Structural Dynamics (MSD). This choice is somehow obliged when dealing with non-linear aeroservoelastic phenomena. The developed high-fidelity toolbox is based on the following free software tools:

- AeroFoam density-based compressible RANS solver, developed at Dipartimento di Ingegneria Aerospaziale of Politecnico di Milano (DIAPM);
- MBDyn multipurpose multibody solver developed at DIAPM;
- Code_Aster Finite Element solver, developed at EDF;

- ScicosLab general purpose block diagram simulator, developed at INRIA.

The free research code MBDyn can originally interact with external solvers via inter-process communication. Similar communication capabilities have been added to the other software tools. In this way, a multidisciplinary environment is built, where all the simulators interact together during runtime, offering the co-simulation layout.

Active control of aeroservoelastic phenomena, especially in the transonic flow regime, is a key technology for the design of future aircraft. The Benchmark Active Controls Technology (BACT) project is part of NASA Langley Research Center Benchmark Models Program for studying transonic aeroservoelastic phenomena. The BACT wind-tunnel model was developed to collect high quality unsteady aerodynamic data (pressures and loads) near transonic flutter conditions and demonstrate the potential of designing and implementing active control systems for flutter suppression using flaps and spoilers [5].

The BACT wind-tunnel model has been used in this work as a reference test case, since a wide database of experimental and numerical results is available. It is expected that nonlinear transonic effects and aerodynamic time delays will have an important role in the dynamic behavior of the system, and Computational Fluid Dynamics will be necessary to tackle the aeroelastic problem [6]. Tackling more complex real world application, such as the nonlinear trim of free-flying aircraft and the design and validation of its flutter suppression control systems, will be a further development of this work.

2 Software Environment

The software environment is composed of different simulators. A snapshot of a typical result obtained by the software described in this work is shown in Figure 1, where the structural and the aerodynamic meshes are shown for a deformed shape of a complete aircraft.

The communication technique chosen to make these simulators interact with each other is based on TCP/IP Internet sockets. This kind of data transmission is very efficient (way more than, for example, employing text file read/write functions), and it is naturally directed to multiple machines layout, which, in many cases, can sensitively decrease the time-to-solution. In such a layout, the local communication is seen as a special subcase of the network-based data exchange. If sockets are used in blocking mode, each process is blocked until all the expected informations are available from the external simulator. In this way, synchronization is automatically ensured.

The layout of the high-fidelity model used in this work is based on the multibody simulator and the aerodynamic RANS solver. A brief description of the two softwares is given in the next sections.

At each time step during the simulation, AeroFoam computes the aerodynamic pressure distribution to output the loads required by MBDyn. These loads are written on the dedicated communication socket. MBDyn reads the loads and solves the nonlinear constrained dynamic problem: the output of this step being displacements and velocities, written again on the same socket. AeroFoam Reads the output from MBDyn, deforms the computational domain and solves again the aerodynamics. These steps are repeated iteratively until the simulation brakes.

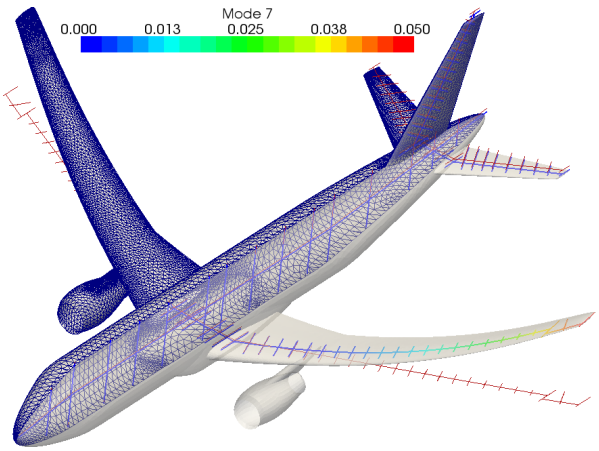

Fig. 1 Typical result of the co-simulation toolbox.

2.1 MBDyn

MBDyn (http://www.mbdyn.org/) is a free general-purpose multibody simulator developed at Dipartimento di Ingegneria Aerospaziale of Politecnico di Milano (DIAPM), Italy. This code solves Initial Value Problems (IVP) using an original formulation based on Newton-Euler equations of motion. The equations of a set of rigid bodies, written in first-order form, as a set of Differential-Algebraic Equations (DAE), with kinematic constrains explicitly enforced using Lagrange's multipliers, are integrated in time using implicit second-order accurate multistep A/L-stable integration algorithms with tunable algorithmic dissipation [7][8] .

The equations of motion of a system of n_b bodies are

$$\mathbf{M}(\mathbf{q})\dot{\mathbf{q}} = \mathbf{p} \tag{1a}$$

$$\dot{\mathbf{q}} + \phi_{/\mathbf{q}}^{T}\lambda = \mathbf{f}(\mathbf{q}), \dot{\mathbf{q}}, \mathbf{p}, t \tag{1b}$$

$$\phi(\mathbf{q}, t) = \mathbf{0} \tag{1c}$$

where the mass matrix $\mathbf{M}$ contains the lumped mass of each body, $\mathbf{q}$ is a set of coordinates that correspond to the position and orientation parameters of the bodies, and $\mathbf{f}$ is a set of time- and configuration-dependent forces acting on the bodies. Vector $\mathbf{p}$ contains the momentum and the momenta moments of the bodies; ϕ are the kinematic constraints, while vector λ contains the related Lagrange's multipliers. The dimension of the problem is $n = 12 \times n_b + c$. At each time step, the constrained dynamic problem is solved by Newton-Raphson iterations, which are performed until convergence is reached.

MBDyn can output a wide variety of signals, corresponding to ideal measurements based on the internal state of a dynamic model, including the value of kinematic coordinates, aggregate information like strains and stresses, possibly filtered by simulated sensor dynamics. This feature is supported by a specific family of elements. At the same time, inputs received by companion software can be used as scaling factors of mechanical loads, imposed motion of actuators, generic input to drivers, and more. This feature is dealt with by a specific family of input handlers.

2.2 AeroFoam

The aerodynamic sub-system is modelled with the Finite-Volume (FV) aerodynamic solver AeroFoam, developed at DIAPM, Italy. It kicked-off back in 2008, as an ambitious academic experiment, which had the challenging target of filling the empty space left in OpenFOAM (no density-based compressible solver were available).

AeroFoam is a density-based compressible RANS (Reynolds Averaged Navier Stokes) solver: it can be considered the optimal layout for transonic industrial applications. It also provides Euler equations modelling options. Among the innovative contributions, it is worthwhile to remark: the dedicated aeroelastic interface scheme based on Moving Least Squares (MLS) interpolation strategy, providing all the functionalities necessary to link the structural sub-system with the aerodynamic one, and the dedicated hierarchical mesh deformation tool for dealing with moving boundary problems in Arbitrary Lagrangian Eulerian (ALE) formulation.

3 Design method of flutter suppression active control system

The design method is presented applied to the BACT wing problem. As shown in Figure 2 the BACT wind-tunnel model is a rigid rectangular wing with a NACA 0012 airfoil section. It is equipped with a trailing-edge control surface and upper and lower-surface spoilers that can be controlled independently by means of hydraulic actuators. The wind-tunnel model is instrumented with pressure transducers, accelerometers, control surface position sensors, and hydraulic pressure transducers. The accelerometers are the primary sensors for feedback control and are located at each corner of the wing. The wing is mounted to a device called the Pitch and Plunge Apparatus (PAPA) which is designed to permit motion in principally two modes, rotation (or pitch) and vertical translation (or plunge). The mass, inertia, and center of gravity location of the system can be controlled by locating masses at various points

along the mounting bracket. The stiffness properties can be controlled by changing the properties of the rods. The PAPA is instrumented with strain gauges to measure normal force and pitching moment and it is mounted to a turntable that can be rotated to control the wing angle of attack. The combination of the BACT wing section and PAPA mount (which will be referred to as BACT system) was precisely tuned to flutter within the operating range of the Transonic Dynamics Tunnel (TDT) at NASA Langley Research Center

The BACT system has a dynamic behavior very similar to the classical 2 d.o.f. wing section. The difference is primarily the complexity of the aerodynamic behavior and the presence of additional structural modes. The finite span and low aspect ratio of the BACT wing introduce significant three-dimensional flow effects. Higher frequency structural degrees of freedom are associated with the PAPA mount and the fact that the wing section is not truly rigid. The control surfaces also introduce complexities not typically reflected in the classical 2 d.o.f. system. The mass and inertia of the control surfaces and potential flexibility in their support structures introduce inertial coupling effects. The finite span of the control surfaces and their close proximity to each other also introduce significant aerodynamic effects. All these issues influence the development of the equations of motion but, as will be seen, do not force the abandonment of the 2 d.o.f. system structure.

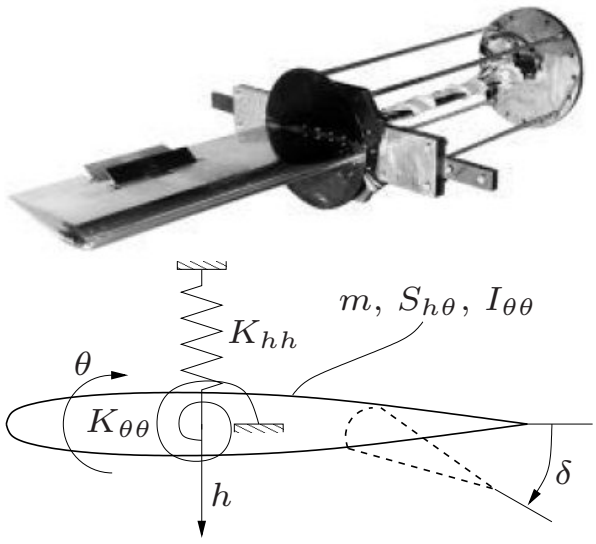

Fig. 2 Experimental set-up for the BACT wing.

The objective of the present work is to design a flutter suppression active control system for the BACT wing to operate within the highly non-linear transonic regime with a linear, low-fidelity but efficient model and then verify the performances with a non-linear, high-fidelity but expensive model (surveying both Euler and RANS modelling options). More precisely we design a simple Proportional-Integral (PI) active control system by means of a multi-objective optimization strategy based on Genetic Algorithms (GA). Successively we compare the results of post-flutter direct simulations with control system on and off with both the low and high-fidelity tools. Preliminarily we stick to a two-dimensional approximation also for the high-fidelity model. Of course further three-dimensional high-fidelity direct simulations are required in order to fully assess the potential of the proposed flutter suppression strategy.

3.1 Low-fidelity model

For the design of active control systems it is convenient to adopt an approximated and efficient numerical model with a small number of d.o.f. providing satisfactory results within the frequency range of interest, rather than choosing an over-detailed and expensive numerical model. To this end the BACT wing and each control surface are assumed to be rigid in both the spanwise and chordwise directions. This assumption is supported by the fact that the wing and control surfaces were constructed to be as rigid as possible. It is also assumed that the motion is limited to the 2 d.o.f. of pitch and plunge. This assumption implies that the other structural modes of the BACT wing are not significant. Investigation of the structural vibration characteristics of the PAPA mount was shown to support this assumption. In fact the next lowest frequency for any transverse mode was more than six times the frequency of the pitch and plunge modes and well outside the frequency range of interest. [5]

Within such a framework the structural model for the BACT wing can be written as the following system of Ordinary Differential Equations (ODE) in the unknown generalized coordinates $\{q(t)\} = \{h(t), \theta(t)\}^{\mathsf{T}}$:

$$[\mathbf{M}]\{\ddot{q}\} + [\mathbf{C}]\{\dot{q}\} + [\mathbf{K}]\{q\} = \{Q_a(t)\} + \{Q_c(t)\}, \tag{2}$$

where the structural mass, damping and stiffness matrices $[\mathbf{M}]$, $[\mathbf{C}]$ and $[\mathbf{K}] \in \mathbb{R}^{2\times 2}$ can be written as follows:

$$[\mathbf{M}] = \begin{bmatrix} m & S_{h\theta} \\ S_{h\theta} & I_{\theta\theta} \end{bmatrix}$$

$$[\mathbf{C}] = \begin{bmatrix} C_{hh} & 0 \\ 0 & C_{\theta\theta} \end{bmatrix} = \begin{bmatrix} 2m\zeta_h\omega_h & 0 \\ 0 & 2I_{\theta\theta}\zeta_\theta\omega_\theta \end{bmatrix}$$

$$[\mathbf{K}] = \begin{bmatrix} K_{hh} & 0 \\ 0 & K_{\theta\theta} \end{bmatrix} = \begin{bmatrix} m\omega_h^2 & 0 \\ 0 & I_{\theta\theta}\omega_\theta^2 \end{bmatrix}, \tag{3}$$

where $m = 88.73$ kg is the mass, $S_{h\theta} = 6.31 \cdot 10^{-2}$ kg m the static unbalance and $I_{\theta\theta} = 3.79$ kg m^2 the moment of inertia of the BACT wing. The structural natural frequencies and damping coefficients for the plunge and pitch d.o.f. respectively are $\omega_h = 21.01$ rad/s, $\omega_\theta = 32.72$ rad/s, $\zeta_h = 1.4 \cdot 10^{-3}$ and $\zeta_\theta = 10^{-3}$.

Similarly the aerodynamic model for the BACT wing is based on a quasi-steady linear(ized) approximation of the array of the Generalized Aerodynamic Forces (GAF) due to structural motion $\{Q_a(t)\}$ and control surfaces deflection $\{Q_c(t)\}$ respectively, with stability and control derivatives computed by means of a Finite Differences (FD) strategy from wind tunnel experimental data measured at $M_\infty = 0.77$ and $q_\infty = 6846.84$ Pa, namely:

$$\{Q_a\} = \frac{L_a^2}{V_\infty^2}[\mathbf{M}_a]\{\ddot{q}\} + \frac{L_a}{V_\infty}[\mathbf{C}_a]\{\dot{q}\} + [\mathbf{K}_a]\{q\}$$

$$\{Q_c\} = [\mathbf{M}_c]\ddot{\delta} + \frac{L_a}{V_\infty}[\mathbf{C}_c]\dot{\delta} + [\mathbf{K}_c]\delta, \tag{4}$$

where the aerodynamic mass, damping and stiffness matrices associated with the structural motion $[\mathbf{M}_a]$, $[\mathbf{C}_a]$, $[\mathbf{K}_a] \in \mathbb{R}^{2\times 2}$ and with the control surfaces deflection $[\mathbf{M}_c]$, $[\mathbf{C}_c]$, $[\mathbf{K}_c] \in \mathbb{R}^{2\times 1}$ can be written as follows:

$$\begin{aligned}
[\mathbf{M}_a] &= q_\infty \frac{2S}{c}\begin{bmatrix} -C_{L/\dot{\alpha}} & -\ell C_{L/\dot{\alpha}} \\ cC_{M/\dot{\alpha}} & c\ell C_{M/\dot{\alpha}} \end{bmatrix} \\
[\mathbf{M}_c] &= -\begin{bmatrix} S_{h\delta} \\ S_{\theta\delta} \end{bmatrix} \\
[\mathbf{C}_a] &= q_\infty \frac{2S}{c}\begin{bmatrix} -C_{L/\alpha} & -\ell C_{L/\alpha} \\ cC_{M/\alpha} & c\ell C_{M/\alpha} \end{bmatrix} \\
[\mathbf{C}_c] &= q_\infty S\begin{bmatrix} -C_{L/\dot{\delta}} \\ cC_{M/\dot{\delta}} \end{bmatrix} \\
[\mathbf{K}_a] &= q_\infty S\begin{bmatrix} 0 & -C_{L/\alpha} \\ 0 & cC_{M/\alpha} \end{bmatrix} \\
[\mathbf{K}_c] &= q_\infty S\begin{bmatrix} -C_{L/\delta} \\ cC_{M/\delta} \end{bmatrix}
\end{aligned} \tag{5}$$

where $c = 0.4053$ m is the chord, $S = 0.3298$ m^2 is the surface and $\ell = -0.1750$ is the relative distance between the elastic axis and the aerodynamic center of the BACT wing. The aerodynamic reference length is here considered equal to half the aerodynamic chord, namely: $L_a = c/2$. Finally the stability and control derivatives evaluated experimentally are tabulated in literature. [5] The need to include more sophisticated aerodynamic modelling options such as unsteady kernel approximations or time accurate CFD is albeit mitigated by the fact that the reduced frequency for the BACT wing is relatively low, approximately $k \simeq 0.05$.

As discussed above the primary objective of the present work is that of assessing the dynamic stability properties of the BACT wing by computing the flutter velocity V_F. More in general it is convenient to investigate the behavior of the eigenvalues of the aeroservoelastic system $s = \sigma + i\omega$ as a function of the the flight velocity V_∞. Below we illustrate the results of the classical non-linear root-tracking procedure for building the $V_\infty - \omega$ and $V_\infty - g$ diagrams as applied to the following matrix, resulting from the quasi-

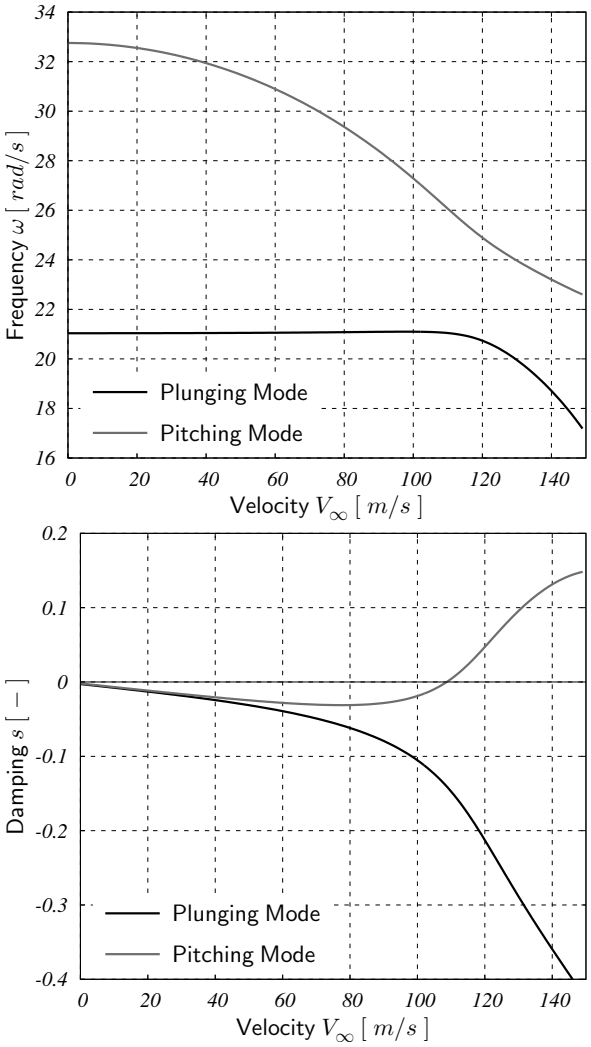

Fig. 3 $V_\infty - \omega$ and $V_\infty - g$ diagrams for the BACT wing.

steady approximation presented above:

$$[\mathbf{A}(s,V_\infty)] = s^2\left([\mathbf{M}] - \frac{L_a^2}{V_\infty^2}[\mathbf{M}_a]\right) + s\left([\mathbf{C}] - \frac{L_a}{V_\infty}[\mathbf{C}_a]\right) + \left([\mathbf{K}] - [\mathbf{K}_a]\right). \tag{6}$$

In Figure 3 the $V_\infty - \omega$ and $V_\infty - g$ diagrams for the BACT wing are presented. It is interesting to observe that near-by the flutter point the bending and torsional frequencies in the $V_\infty - \omega$ diagram tend to coalesce. The pitching mode is unstable yielding an open-loop flutter velocity $V_F^{\mathsf{OL}} = 108.66$ m/s almost perfectly matching with the reference value available in literature $V_F^{\mathsf{Exp}} = 108.57$ m/s. [5]

3.2 Active control system design

The secondary objective of the present work is to design a flutter suppression active control system for the BACT wing, e.g. in such a way that the flutter velocity V_F is increased by $10\% - 15\%$. From a regulatory point of view such an achievement is highly favorable since it is necessary to demonstrate flutter clearance within a flight envelope expanded by 15% on V_D.

More precisely we choose a very simple active control system architecture based on a Proportional-Integral (PI) feedback of the flap control surface, which can be represented as follows within the frequency domain:

$$\delta = \left([\mathbf{D}_P] + \frac{1}{s}[\mathbf{D}_I]\right)\{q\} \tag{7}$$

where the proportional and integral gain matrices $[\mathbf{D}_P]$, $[\mathbf{D}_I] \in \mathbb{R}^{1\times 2}$ are unknown. It is now possible to assess the closed-loop dynamic stability properties of the BACT wing by means of the non-linear root-tracking procedure as applied to the following matrix, resulting from the additional contributions associated with the active control system:

$$[\mathbf{B}(s,V_\infty,[\mathbf{D}_P],[\mathbf{D}_I])] = [\mathbf{A}(s,V_\infty)] - \left(s^2[\mathbf{M}_c] + s\frac{L_a}{V_\infty}[\mathbf{C}_c] + [\mathbf{K}_c]\right)[\mathbf{D}_P] - \left(s[\mathbf{M}_c] + \frac{L_a}{V_\infty}[\mathbf{C}_c] + \frac{1}{s}[\mathbf{K}_c]\right)[\mathbf{D}_I]. \tag{8}$$

The unknown proportional and integral gain matrices $[\mathbf{D}_P]$, $[\mathbf{D}_I]$ should be computed in such a way that the stability of the pitching mode is increased while the stability of the pitching mode is unaltered. In other terms the $V_\infty - g$ diagram of the closed loop aeroservoelastic system should match as closely as possible a user's defined target $V_\infty - g^{\mathsf{Tgt}}$ diagram. Such a task is not trivial since we are not focusing on a single flight condition but we are trying to design

an active control system robust enough to provide the desired stability augmentation capabilities on the whole flight envelope. With reference to Figure 5 we resort to a multi-objective optimization strategy based on Genetic Algorithms (GA). The unknown proportional and integral gain matrices $[\mathbf{D}_P]$, $[\mathbf{D}_I]$ are computed solving an evolution-like problem, minimizing the following weighted-sum functional:

$$\mathcal{J}([\mathbf{D}_P],[\mathbf{D}_I]) = \frac{1}{2}\frac{\|g-g^{\mathsf{Tgt}}\|^2}{\|g^{\mathsf{Tgt}}\|^2} + \frac{1}{2}\frac{\|[\mathbf{D}_P]\|^2}{D_{\mathsf{Max}}^2} + \frac{1}{2}\frac{\|[\mathbf{D}_I]\|^2}{D_{\mathsf{Max}}^2}, \tag{9}$$

where the first term is related to stability augmentation while the other terms are related to active control system energy attenuation. The knob D_{Max} can be used to adjust the relative weight between these two opposing requirements.

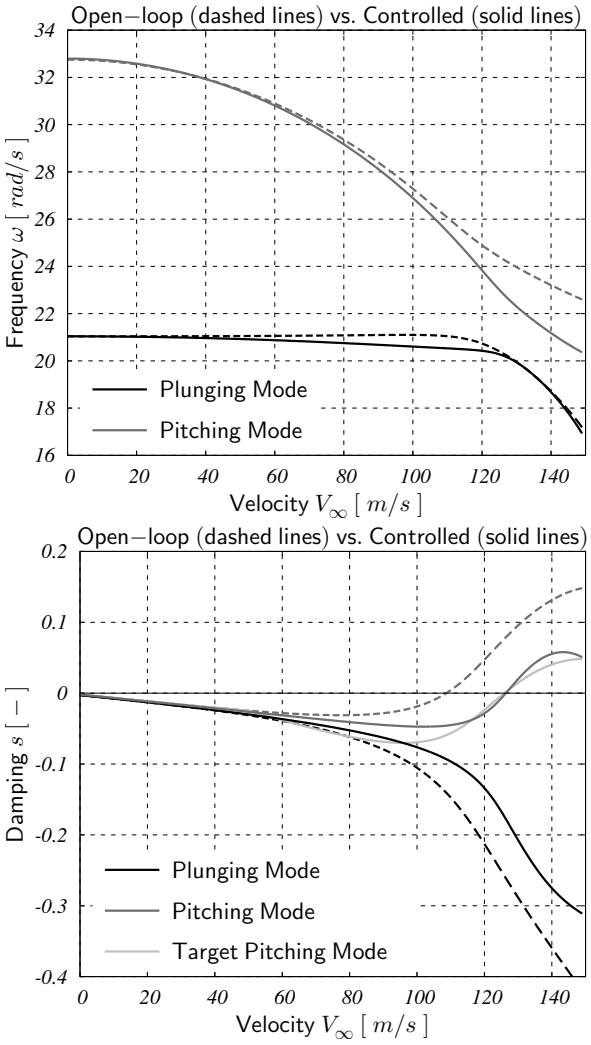

Fig. 4 Closed-loop $V_\infty - \omega$ and $V_\infty - g$ diagrams for the BACT wing.

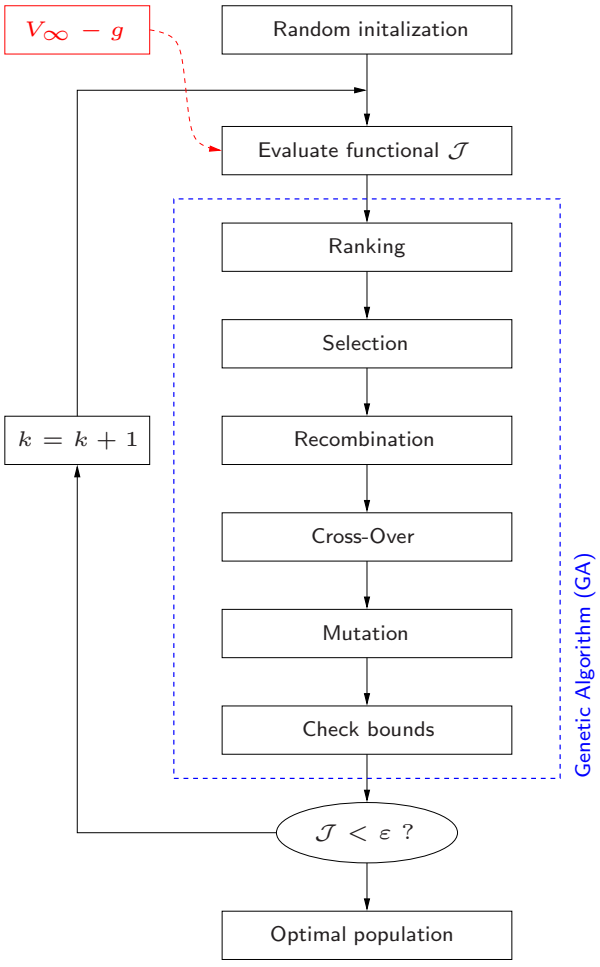

Fig. 5 Genetic optimization block diagram for the BACT wing.

3.3 High-fidelity model

The final objective of the present work is to verify the performances of the designed flutter suppression active control system for the BACT wing by means of a non-linear, high-fidelity but expensive model (surveying both Euler and RANS modelling options). Preliminarily we stick to a two-dimensional approximation also for the high-fidelity model. Of course further three-dimensional high-fidelity direct simulations are required in order to fully assess the potential of the proposed flutter suppression strategy. To this end we repeat with a high-fidelity non-linear model the post-flutter direct simulations presented above for a low-fidelity linear model with control system on and off. This strategy yields a significant added value to the workflow since it makes possible to appreciate how important the neglected non-linear effects actually are and therefore the robustness of the designed active control system.

4 Numerical Results

4.1 Low-fidelity model results

In Figure 4 the closed-loop $V_\infty - \omega$ and $V_\infty - g$ diagrams for the BACT wing are compared with the open-loop and with the user's defined target ones. It is remarkable that the stability of the plunging mode is minimally altered while the stability of the pitching mode is significantly augmented with a closed-loop flutter velocity of $V_F^{\mathsf{CL}} = 126.37\ \mathrm{m/s}$, more or less 15% higher than the open-loop value.

Besides the the analysis of the stability properties, it is also convenient to run a numerical simulation formally identical to a wind-tunnel or in-flight experimental campaign. Such a "direct simulation" procedure paves the way for the investigation more in detail of the behavior of the BACT wing near-by the flutter point. To this end it is possible to perform a deep-dive on how the robustness of the active control system is affected by the sensors (mono-directional accelerometers) and actuators (hydraulic servo-systems with saturation set at $\overline{\delta} = 12^\circ$) modelled with reference to experimental data. Moreover the effects of the digital realization of the active control system are also modelled by including a pseudo-integrator to reconstruct the position given the outputs of the accelerometers and an anti-aliasing analogic filter.

In Figures 6 and 7 the numerical results of the direct simulations of the open-loop and closed-loop (with the designed PI active control system active) behavior of the BACT wing are presented. Firstly it is possible to observe that beyond the open-loop flutter velocity $V_F^{\mathsf{OL}} = 108.66\ \mathrm{m/s}$ the BACT wing is unstable to a small perturbation of the initial condition of the pitch angle $\theta_0 = 2^\circ$, with both plunge and pitch d.o.f. rapidly

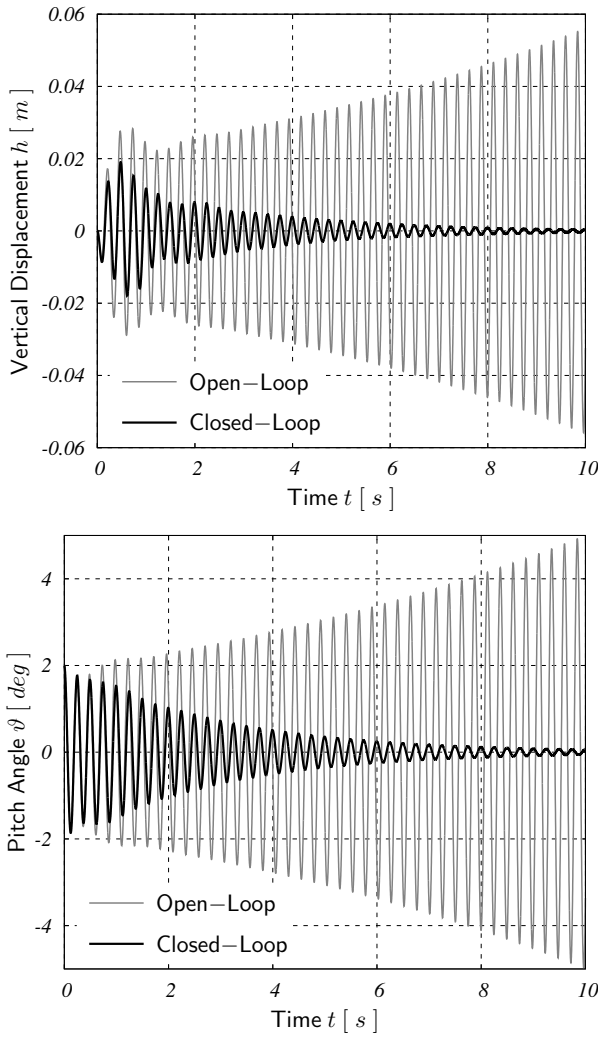

Fig. 6 Vertical displacement h (top) and pitch angle θ (bottom) at $V_\infty = 1.05 V_F^{\mathsf{OL}}$.

diverging to infinity together with the total energy. Viceversa when the active control system is switched on it is possible to verify the robustness of the designed PI feedback law. In fact both both plunge and pitch d.o.f. rapidly converge to zero together with the total energy. Finally in Figure 8 the time history of the flap deflection corresponding to the designed active control system law is presented for analogic or digital implementations. It is interesting to highlight the saturation of the hydraulic actuators at $\overline{\delta} = 12°$, occurring within the first time instants. Moreover it is worthwhile to remark the significant time delay between the numerical results associated with an analogic implementation and a more realistic digital implementation (including within the verification model also the anti-aliasing analogic filter).

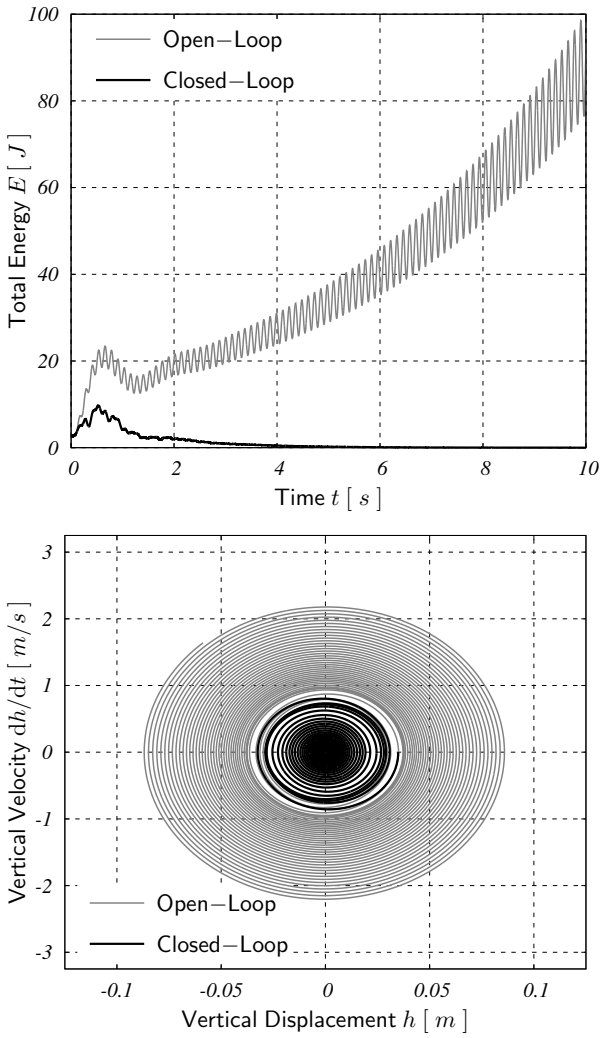

Fig. 7 Total energy E (top) and phase-space plot (bottom) at $V_\infty = 1.05V_F^{\mathrm{OL}}$.

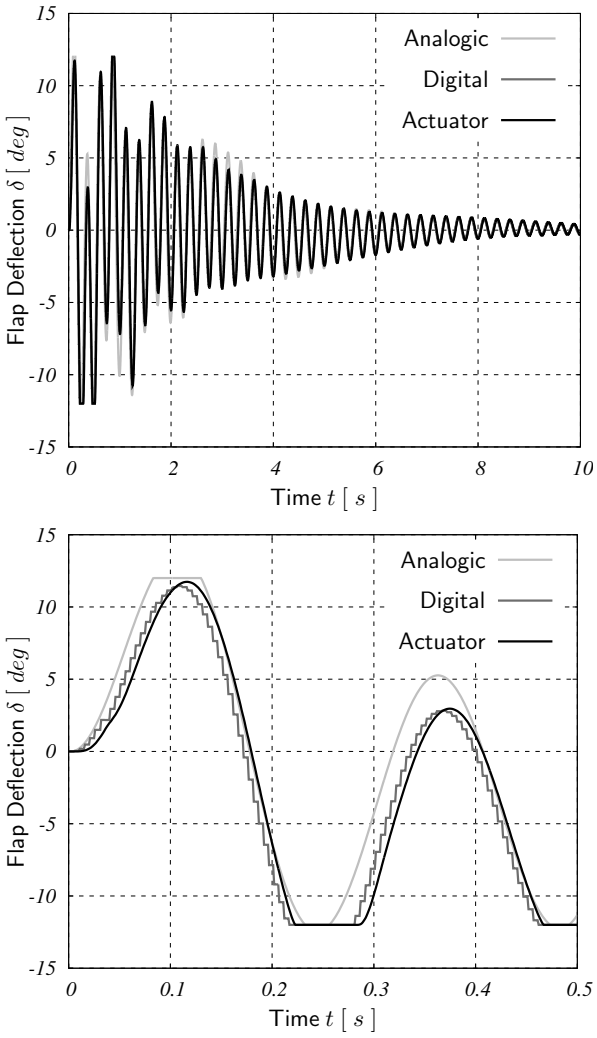

Fig. 8 Flap deflection δ (top) together with a zoom (bottom) at $V_\infty = 1.05V_F^{\mathrm{OL}}$.

4.2 High-fidelity model results

In Figure 9, the pressure distribution relative to an instant of the simulation is shown. In Figure 10 the numerical results of the direct simulations of the open-loop and closed-loop behavior of the BACT wing computed with the low-fidelity model are compared with those of the high-fidelity model. Firstly it is interesting to observe that the open-loop responses are significantly different, with the pitch angle time history predicted by the high-fidelity model diverging

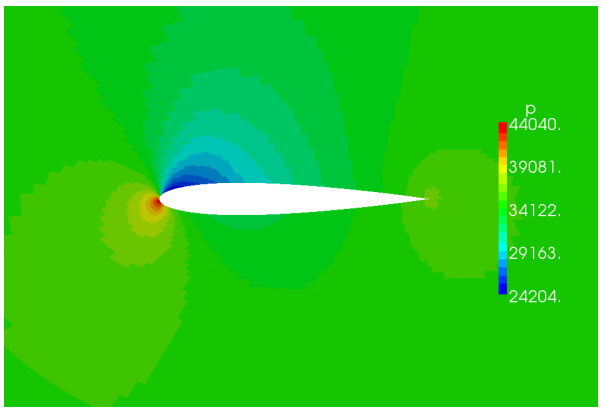

Fig. 9 Pressure distribution computed by AeroFoam.

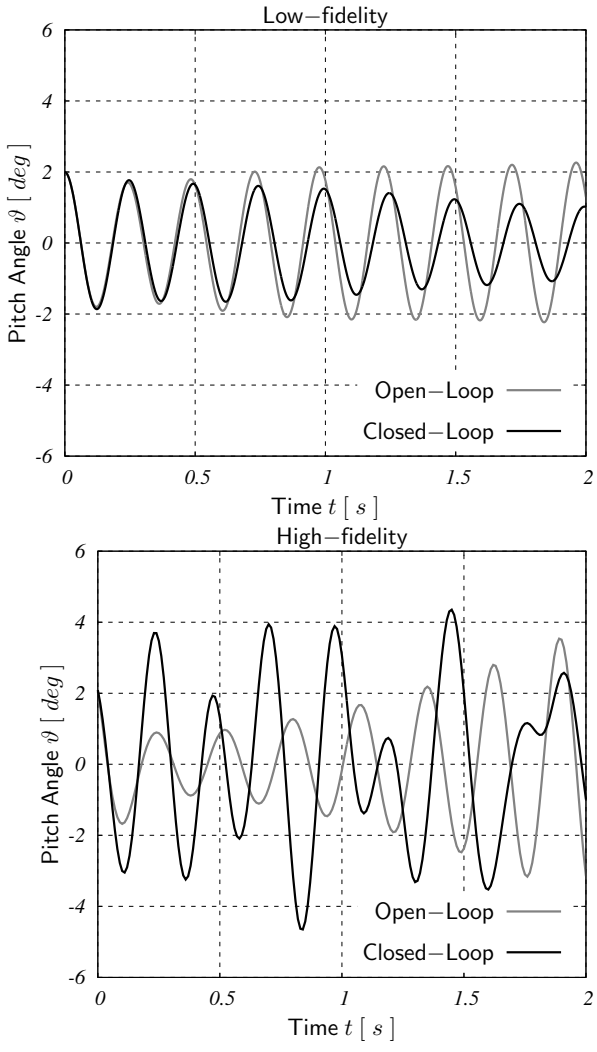

Fig. 10 Pitch angle θ compared between low-fidelity (top) and high-fidelity (bottom) models.

much more rapidly than the low-fidelity model (with maximum amplitude almost doubled at $t =$ 2 s). Moreover it is worthwhile to stress that the closed-loop responses do not provide encouraging insights on the robustness of the designed active control system. In fact, within the high-fidelity framework the active control system is not robust enough to drive the total energy of the system to zero as observed within the low-fidelity framework. On the contrary the PI feedback only limits the total energy below a rather high threshold with $\Delta\theta \simeq \pm 4^\circ$. The main effects not taken into account by the low-fidelity model are:

- nonlinearities brought by shock waves;
- time delays.

5 Conclusions and future work

Together with the availability of more and more powerful computing resources, current trends pursue the adoption of high-fidelity tools and state-of-the-art technology within the very active and fruitful research fields of Computational Structural Dynamics (CSD), Multibody System Dynamics (MSD) and Computational Fluid Dynamics (CFD). This choice is somehow obliged when dealing with non-linear aeroservoelastic phenomena, such as transonic flutter, aileron buzz and buffeting.

In the present work we present a multi-fidelity approach to design a flutter suppression active control system, operating in transonic regime. At the high-fidelity level, our purpose has been to use a free software co-simulation environment for solving multidisciplinary non-linear Fluid-Structure Interaction (FSI) problems with a partitioned approach, that is coupling high-fidelity state-of-the-art CSD/MSD and CFD tools, and eventually active control modelling tools.

It has been shown that the high-fidelity model leads to different conclusions about the feasibility of the design, even for a relatively simple problem, as the BACT wing is. This is due to the neglected nonlinear effects, that are typically not taken into account in approximated design models. This results underlines the need to adopt realistic high-fidelity simulations and analysis tools

to verify the system performances, and eventually modify the design.

The integration of the proposed layout in the design process of a transonic flutter control system can lead to more precise predictions of the real system behavior, which reduce the experimental tests, and thus costs and time-to-market.

The approach followed in this work can also drive some enhancements to apply to the low-fidelity model, in order to build an intermediate level of approximation. In this case, for instance, it could be possible to add shock waves nonlinearities and time delays, to be tuned based on the CFD simulations.

A natural development of this work is the implementation of an optimization loop based on the high-fidelity model, in order to offer a more robust and efficient design process. Also, future works will focus on more complex industrial applications, such as the nonlinear trim of free-flying aircraft and the design and validation of its flutter suppression control systems.

References

[1] A. J. Ostroff, K. D. Hoffler, and M. S. Proffitt, "High-Alpha Research Vehicle (HARV) Longitudinal Controller: Design, Analyses, and Simulation Results", *NASA Technical Paper 3446*, 1994

[2] K. J. Badcock, S. Timme, S. Marques, H. Khodaparast, M. Prandina, J. E. Mottershead, A. Swift, A. Da Ronch, and M. A. Woodgate, "Transonic aeroelastic simulation for instability searches and uncertainty analysis", *Progress in Aerospace Sciences*, 2011

[3] K. Becker and J. Vassberg, "Numerical Aerodynamics in Transport Aircraft Design", *Notes on Numerical Fluid Mechanics*, 2009

[4] M. J. de C. Henshaw, K. J. Badcock, G. A. Vio, C. B. Allen, J. Chamberlain, I. Kaynes, G. Dimitriadis, J. E. Cooper, M. A. Woodgate, A. M. Rampurawala, D. Jones, C. Fenwick, A. L. Gaitonde, M. A. Taylor, D. S. Amor, T. A. Eccles, and C. J. Denley, "Non-linear Aeroelastic Prediction for Aircraft Applications", *Progress in Aerospace Sciences*, 2007

[5] M. R. Waszak, "Modeling the Benchmark Active Control Technology Wind Tunnel Model for Application To Flutter Suppression", *AIAA Technical Paper 3437*, 1996.

[6] R. M. Bennet and J. W. Edwards, "An overview of recent developments in computational aeroelasticity", *Proceedings of the 29^{t}h AIAA Fluid Dynamics Conference*, 1998.

[7] G. Ghiringhelli, P. Masarati, P. Mantegazza, and M. W. Nixon, "Multi-body analysis of a tiltrotor configuration", *Nonlinear Dynamics, 19(4):333âĂŞ357*, 1999

[8] P. Masarati, M. Lanz, and P. Mantegazza, "Multistep integration of ordinary, stiff and differential-algebraic problems for multibody dynamics applications", *XVI Congresso Nazionale AIDAA, Palermo*, 24âĂŞ28 September 2001.

Copyright Statement